END-PLATE MOMENT CONNECTIONS: TEST RESULTS AND FINITE ELEMENT METHOD VALIDATION

Emmett A. Sumner, Timothy W. Mays, and Thomas M. Murray
Department of Civil and Environmental Engineering
Virginia Polytechnic Institute
Blacksburg, Virginia 24061, USA

ABSTRACT

A series of tests on the four bolt extended unstiffened and the eight bolt extended stiffened moment end-plate connections and a validation study utilizing the finite element method were conducted as a part of the SAC Steel Project. The connections were “heavy” beam-to-column connections between large hot-rolled members that included W24, W30, and W36 beams attached to W14 columns. It was determined that the extended moment end-plate connections can be designed to provide a great deal of ductility in seismic force resisting moment frames and that the finite element method can be used to predict the behavior of end-plate connections.

INTRODUCTION

A great deal of research on the behavior and design of steel seismic load resisting moment frames has been conducted over the past several years. The primary areas of research have been on welded connections and on finding alternative connections that provide adequate ductility. The extended moment end-plate connection is one alternative that has been investigated. As a part of the SAC Steel Project, a series of full-scale beam-to-column extended moment end-plate connection tests and a validation study utilizing the finite element method have been conduced at Virginia Polytechnic Institute and State University. The primary objective of the research program was to determine the suitability of the extended moment end-plate connections for use in seismic force resisting moment frames.

Moment end-plate connections consist of a plate that is shop-welded to the end of a beam that is then field bolted to the connecting member. The connections are primarily used to connect a beam to a column or to splice two beams together. The four bolt extended unstiffened and the eight bolt extended stiffened moment end-plate configurations are the subjects of this paper. The four bolt extended unstiffened end-plate connection consists of two rows of two bolts for each flange. One row is outside the flange on the extended part of the end-plate and the other is inside the flange. The eight bolt extended stiffened end-plate connection consists of four rows of two bolts for each flange. Two rows are outside the flange on the extended part of the end-plate and the other two are inside the flange. The extended part of the end-plate is stiffened by a triangular stiffener centered over the web of the beam. Typical configurations for both connections are shown in Figure 1.

The four bolt extended unstiffened and eight bolt extended stiffened end-plate assemblies were tested under cyclic loading in accordance with the *Protocol for Fabrication, Inspection, Testing, and Documentation of Beam-column Connection Tests and Other Experimental Specimens*, SAC (1). The connections were "heavy" connections between large hot-rolled shapes. Four beam and column combinations were used: W24x68 beam and W14x120 column, W24x68 beam and W14x257 column, W30x99 beam and W14x193 column, and W36x150 beam and W14x257 column. The beam and column members were ASTM A572 Grade 50 steel and the end-plates were ASTM A36 steel. All connections were made with 1 1/4 in. diameter ASTM A325 or ASTM A490 bolts. For each beam and column combination, two end plate configurations were tested. One test was with the connection designed to develop 110 percent of the nominal plastic moment strength of the beam (strong plate connection). The other connection test was designed to develop 80 percent of the nominal plastic moment strength of the beam (weak plate connection). To investigate the effects of a composite slab on the behavior of the connection, one test was conducted using the four bolt extended unstiffened strong plate connection with a 5 in. composite slab cast onto the top flange of the beam. The test matrix for this series of tests is shown in Table 1.

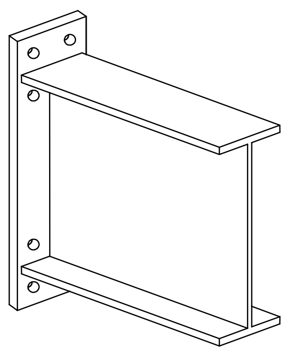

a) Four bolt unstiffened

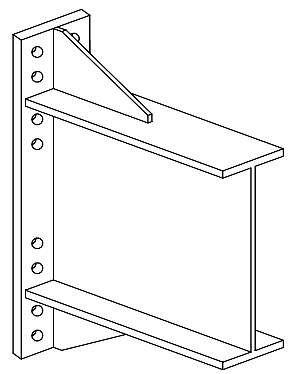

b) Eight bolt stiffened

Figure 1: Extended end-plate connection configurations

DESIGN OF SPECIMENS

The design of the test specimens was done utilizing existing design methods for connections subject to monotonic static loading. The design procedure for the four bolt extended unstiffened connections uses a combination of yield line analysis for determination of the end-plate thickness and the modified Kennedy method, Murray (2); Kennedy et. al. (3) for the calculation of bolt forces. The Kennedy method is based on the “split-tee” analogy, which predicts the forces on the bolts including the effects of prying action. The design of the eight bolt extended stiffened connections was done using the detailed design procedure provided in the AISC Design Guide *Extended End-Plate Moment Connections,* Murray (4). The design guide procedure provides equations for the required plate thickness, based on strength and stiffness, and the determination of bolt forces including the effects of prying action. The equations were developed from regression analyses of data generated by the finite element method. The expected failure mode of the strong plate specimens was local flange and web buckling of the beam and the expected failure mode of the weak plate specimens was end-plate yielding followed by bolt rupture. The column side of the connections was designed in accordance with the *AISC LRFD Manual of Steel Construction,* AISC (5) and the *AISC Seismic Provisions for Structural Steel Buildings,* AISC (6). The columns usually had continuity plates in line with both connecting beam flanges and a web doubler plate attached to one side of the web. The thickness of the continuity plates was approximately equal to the thickness of the connecting beam flanges.

Table 1: Test matrix

Specimen Identification*	Beam / Column	No. of Connection Bolts** (Material)	End-Plate Thickness (in)
4E-1 1/4 -1 1/2-24	W24x68 / W14x120	8 (A490)	1 1/2
4E-1 1/4-1 1/8-24	W24x68 / W14x120	8 (A325)	1 1/8
4E-1 1/4-1 3/8-24 with 5 in. composite slab	(2) W24x68 / W14x257	8 (A490)	1 3/8
8ES-1 1/4-1 3/4-30	W30x99 / W14x193	16 (A490)	1 3/4
8ES-1 1/4-1-30	W30x99 / W14x193	16 (A325)	1
8ES-1 1/4-2 1/2-36	W36x150 / W14x257	16 (A490)	2 1/2
8ES-1 1/4-1 1/4-36	W36x150 / W14x257	16 (A325)	1 1/4

* 4E designates a four bolt extended unstiffened connection
8ES designates an eight bolt extended stiffened connection
** 1 1/4 in. diameter

FABRICATION OF SPECIMENS

The test specimens were fabricated by a combination of university laboratory personnel and commercial fabricators. The end-plate to beam connection was made using complete joint penetration groove welds for the flanges and fillet welds for the web. All welds were made in accordance with the *AWS Structural Welding Code,* AWS (7) using the Flux Cored Arc Welding (FCAW) process and E71T-1 welding electrodes. The flange welds were similar to AWS TC-U4b-GF utilizing a full depth 45-degree bevel and a minimal root opening, backed by a 3/8 in. fillet on the inside of the flanges. The root of the flange groove welds was backgouged after installation of the 3/8 in. fillet to remove any contaminants present from the fillet weld. As recommended by Meng and Murray (8), weld access holes were not used. The beam web to end-plate connection consisted of 5/16 in. fillet welds on both sides of the web. Noteworthy is that the welding procedure used in the fabrication of the test specimens results in an area of non-inspected flange groove weld above the web of the beam. For the eight bolt extended stiffened connections, the stiffener to end-plate and stiffener to beam flange welds were complete joint penetration groove welds. All welds were inspected in accordance with AWS specifications, AWS (7).

TESTING

The primary test setup used in the evaluation of the connections consisted of an exterior beam-column subassemblage with a single cantilever beam attached to the flange of a column. The tests were conduced in a horizontal position to allow use of the available reaction floor supports and for safety of testing. The typical test setup is shown in Figure 2. Lateral supports were provided for the beam at a spacing close enough to prevent lateral torsional buckling of the beam prior to development of its nominal plastic moment strength. A roller was used to support the beam tip and to eliminate any bending moments caused by gravity forces perpendicular to the plane of loading. The load was applied to the free end of the beam using a double acting hydraulic ram. No axial load was applied to the column.

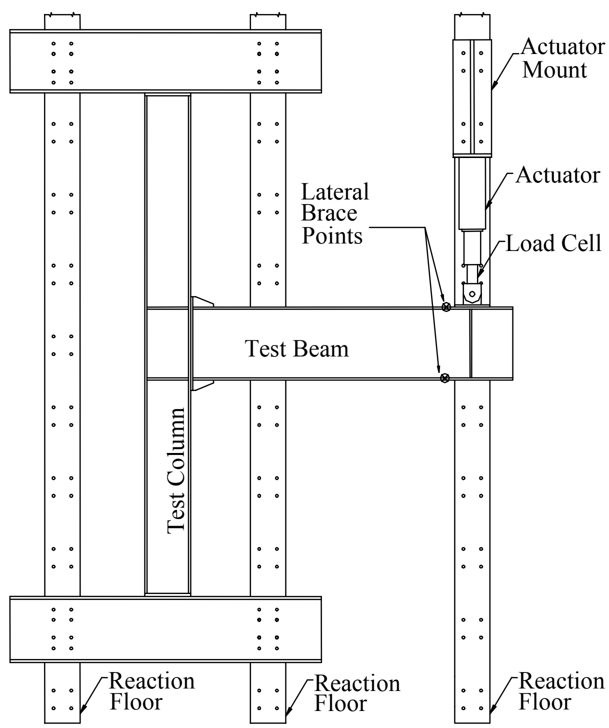

Figure 2: Plan view of test setup

Instrumentation of the test setup included a 200 kip tension-compression load cell, displacement transducers to measure the beam displacement at the point of loading, displacement transducers aligned with the column continuity plates to measure the rotation of the column at the connection, displacement transducers to measure the panel zone rotation, instrumented calipers to measure end-plate separation from the column flange, strain gages to measure the beam and column flange strains, and strain gage rosettes to measure the panel zone strains. Additional displacement transducers were used to measure any rigid body movements of the column ends due to shifting of the test frame. All of the connection bolts were instrumented with strain gages that were installed inside the unthreaded portion of the bolt. The bolts were calibrated prior to testing to establish the load-strain relationship for each bolt. This allowed for accurate tightening of the bolts during assembly of the connection and monitoring of the bolt strains during testing.

The four bolt extended unstiffened connection test with a composite slab was an interior beam-column subassemblage with two cantilever beams attached to opposite flanges of a single column. The test was conducted in a vertical position and utilized W24x68 beams and a W14x257 column. The test setup is shown in Figure 3. The base of the column was supported by a clevis pin assembly attached to support frame beams. The ends of the beams were supported by pinned-end rigid links consisting of a hydraulic ram and a tension-compression load cell attached to support frame beams. The load was applied to the free end of the column using a double acting hydraulic ram. No axial load was applied to the column. Lateral supports were provided at the ends of the beams beyond the support points and at the top of the column at the loading point. Instrumentation of the test setup was similar to the previously described tests.

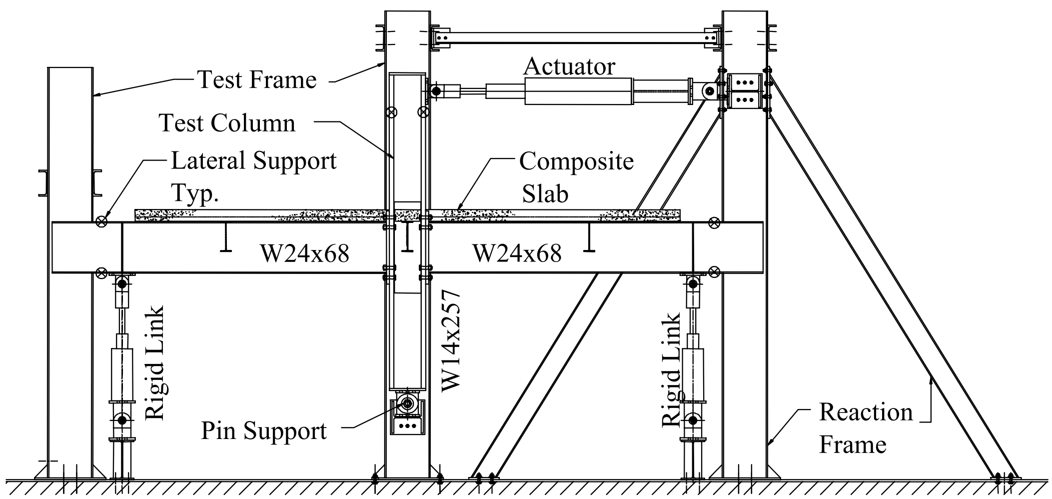

Figure 3: Elevation of slab test setup

Prior to testing, the connection bolts were tightened to the minimum pretension specified in the *AISC LRFD Specification,* AISC (5). The specimen was then whitewashed to aid in the observation of yielding within the connection region. The instrumentation was then reset and the loading was applied. The specimen was loaded in a quasi-static or "slow cyclic" manner in accordance with the *SAC Loading Protocol,* SAC (1). The loading protocol is based on the total interstory drift angle of the beam-column assembly. The interstory drift angles can be achieved by displacing either the beam tip or the column tip. In the horizontal connection tests, a hydraulic ram was used to displace the beam tip until the rotation angles specified by the loading protocol were achieved. In the vertical composite slab test, the column tip was displaced. Any rigid body rotation of the subassemblage due to shifting of the test frame was monitored and subtracted from the total rotation to ensure that the proper rotation angle was achieved. Data points were recorded at regular intervals throughout the duration of the test using a PC-based data acquisition system.

EXPERIMENTAL RESULTS

The six bare steel extended end-plate connection specimens behaved as expected. The strong plate connections (110% of the beam strength) resulted in failure of the beam, local flange and web buckling, with little or no distress observed within the connection region. The weak plate connections (80% of the beam strength) resulted in failure of the connection with one exception, the W30x99 weak plate eight bolt extended stiffened connection (8ES-1.25-1-30) resulted in failure of the beam. The four bolt extended unstiffened connection test with the composite slab did not behave as expected. The beam connections were strong plate connections, which initially resulted in local flange buckling of the beam bottom flanges, but ultimately resulted in tension rupture of the bottom flange bolts.

With the exception of the composite slab test, the strong plate specimens exhibited a great deal of ductility and energy dissipation capacity. Beam flange local buckling, the primary failure mode, is a predictable limit state that provides a ductile failure mechanism. There was no yielding or other distress of the connection region observed during the tests, which indicates that the strong plate connections remained elastic throughout the duration of the test. The total interstory drift rotations that were sustained for at least one complete loading cycle for the strong plate tests ranged from 0.050 to 0.060 radians. The maximum inelastic rotations that were sustained for at least on loading cycle ranged from 0.028 to 0.038 radians. Typical moment vs. total rotation and moment vs. inelastic rotation plots for the strong plate tests are shown in Figure 4.

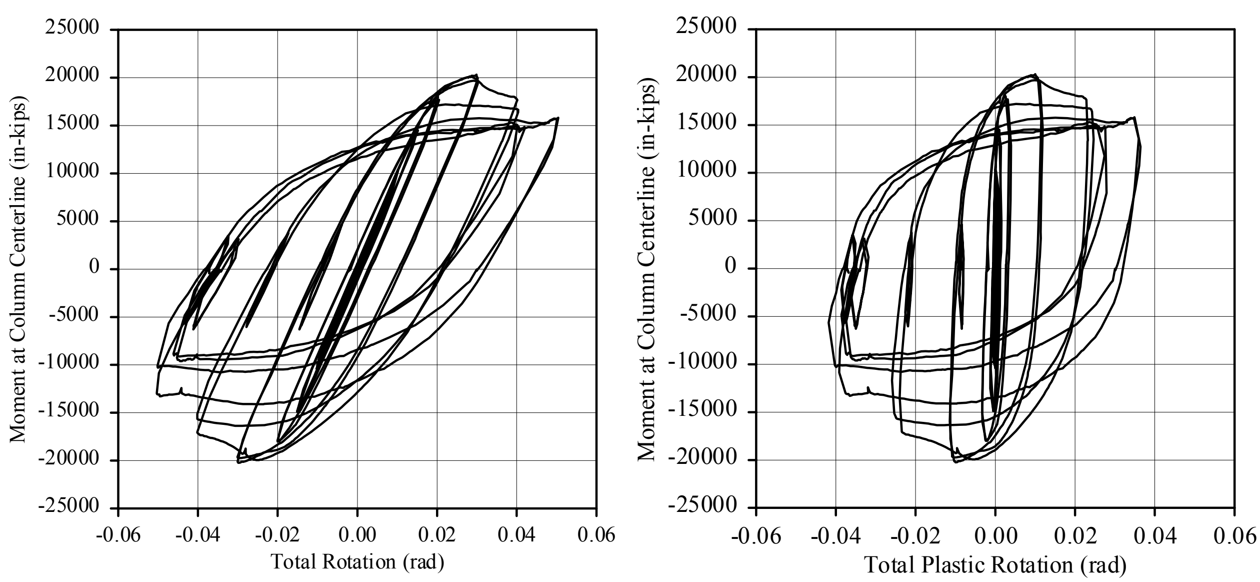

a) Moment vs. Total Rotation b) Moment vs. Total Plastic Rotation

Figure 4: Typical plots of the specimen response (8ES-1.25-1.75-30)

The four bolt extended unstiffened connection test with the composite slab exhibited a moderate about of ductility prior to its brittle failure. The bottom flanges of both beams buckled and then the bottom flange connection bolts ruptured in subsequent cycles. The total interstory drift rotations of the assembly were +0.075 / -0.051 radians which corresponds to inelastic rotations of +0.053 / -0.030 radians.

As expected, the weak plate tests did not exhibit as much ductility as the strong plate tests. The behavior of the weak plate connections was controlled by yielding of the end-plates followed by bolt rupture. In some cases, yielding of the connection region was observed as early as the third load step (0.0075 radians). These controlling limit states are more variable than the beam failure and ultimately result in brittle failure mechanisms. The total sustained interstory drift rotations for the weak plate tests ranged from 0.030 to 0.056 radians with sustained inelastic rotations greater than 0.011 radians.

The behavior of the bolts was of particular interest during the testing. The bolts in the strong plate tests gradually lost the majority of their pretension force as the load cycles increased in magnitude. The maximum observed bolt strains for these connections were only slightly higher than the initial pretension strains. A typical bolt strain vs. moment plot for a strong plate connection is shown in Figure 5a. The weak plate connection bolts were observed to have strains rising sharply above the initial pretension strains as the load steps increased in magnitude. At the higher load steps, the bolts would yield as indicated by permanent set of the bolt strains. As the bolts approached failure, the bolt strains increased very sharply exceeding the range of the strain gages. A typical bolt strain vs. moment plot for a weak plate connection is shown in Figure 5b. Noteworthy is that there were no observed differences in ductility or behavior of the A325 and A490 bolts.

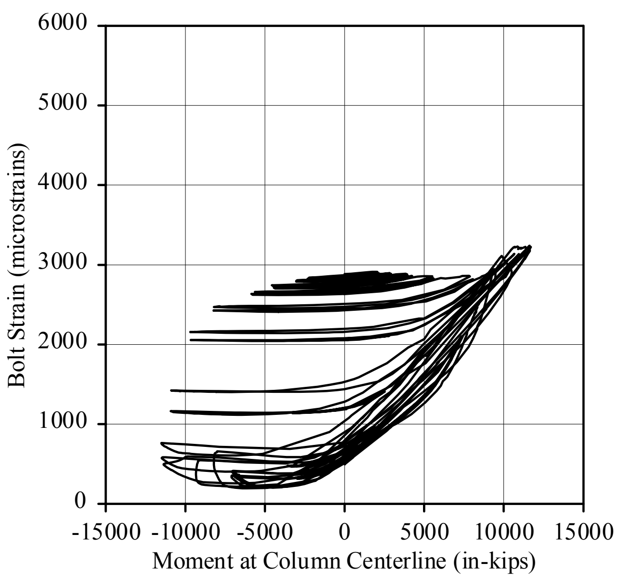

a) Strong plate connection

(8ES-1 1/4-1 3/4-30)

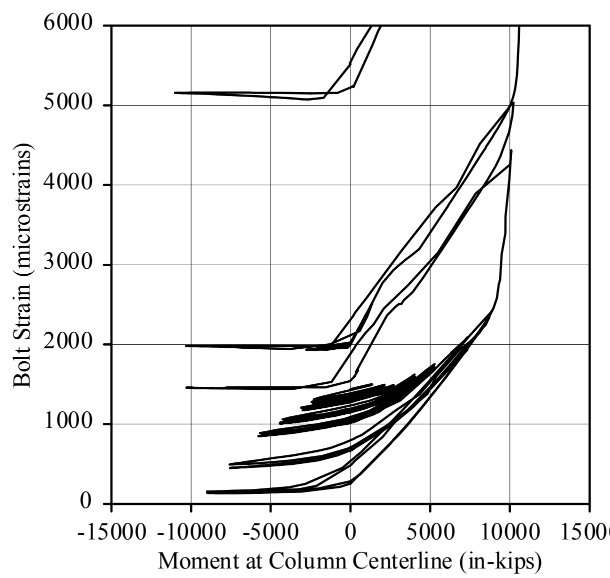

b) Weak plate connection

(4E-1 1/4-1 1/8-24)

Figure 5: Typical bolt strain vs. applied moment plots

A summary of the test performance is shown Table 2. A photograph of a typical beam failure is shown in Figure 6a. The local flange buckling and severe yielding of both flanges and the web is visible. A typical connection failure is shown in Figure 6b. The severe yielding of the end-plate around the bolts and flange is clearly shown.

Table 2: Summary of test performance

Test Identification		M_{max} / $M_{n\ BEAM}$*	θ Total Sustained (rad)	θ P Max Sustained (rad)
4E-1 1/4-1 1/2-24 (Strong Plate)		1.00	0.052	0.038
4E-1 1/4-1 1/8-24 (Weak Plate)		0.95	0.040	0.021
4E-1 1/4-1 3/8-24 with 5" composite slab (Strong Plate)	North Beam	1.28	0.050	0.025
	South Beam	1.27	0.060	0.035
8ES-1 1/4-1 3/4-30 (Strong Plate)		1.00	0.050	0.036
8ES-1 1/4-1-30 (Weak Plate)		1.06	0.056	0.039
8ES-1 1/4-2 1/2-36 (Strong Plate)		1.06	0.050	0.028
8ES-1 1/4-1 1/4-36 (Weak Plate)		0.89	0.030	0.011

* M_{max} = Maximum applied moment at the face of column

$M_{n\ BEAM} = R_y [(F_y + F_u)/2] Z_x = 1.1[(50+65)/2] Z_x$

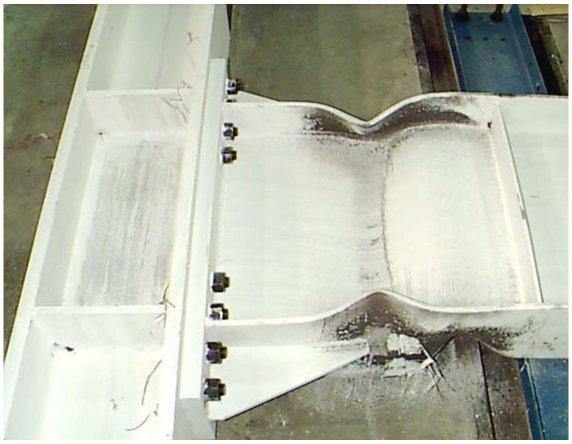

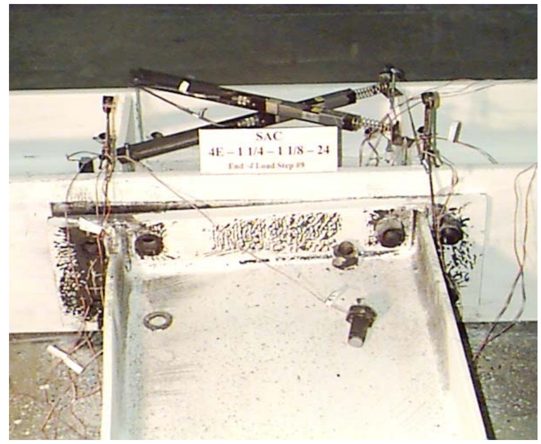

a) Strong plate connection (8ES-1 1/4-1 3/4-30)

b) Weak plate connection (4E-1 1/4-1 1/8-24)

Figure 6: Photographs of typical failures

FINITE ELEMENT MODELING

Current design practice in the United States requires that steel connections that are part of seismic lateral force resisting systems be tested prior to use. However, proper use of the finite element method may provide a basis for justifying a connection configuration for seismic design use. To examine this possibility, finite element models were developed and the results compared to results from several of the tests. The 4E-1 1/4-1 1/8-24 specimen results are reported here. Additional analyses and more detailed results are found in Mays (9).

The ANSYS finite element program was used to model the connection. Solid eight-node brick elements that include plasticity effects were used to model the beam section and column flange. Solid twenty-node elements were used to model the bolts and end-plate. Symmetry about the beam web centerline was used. Contact elements were included between the end-plate and the rigid column flange to model movement of the end-plate away from the column flange. The loading at the end of the beam cantilever matched the "backbone" curve of the experimental results. Prying forces and plastic behavior in the bolts were tracked until divergence occurred due to numerical instability.

Figure 7 shows a portion of the finite element model and the Von Mises stress distribution at the tension flange region. The Von Mises stresses show are for an applied moment of 10,080 in-kips, which closely corresponds to the maximum applied moment of 10,600 in-kips from the experimental test. For this model the beam material yield stress was taken an assumed value of 55 ksi and the end-plate material at the measured value of 37.9 ksi. The beam flange stresses in Figure 7a indicate that yielding has not occurred; however the end-plate material yield stress is exceeded as shown in Figure 7b.

a) Beam-to-column flange connection

b) Isolated end plate

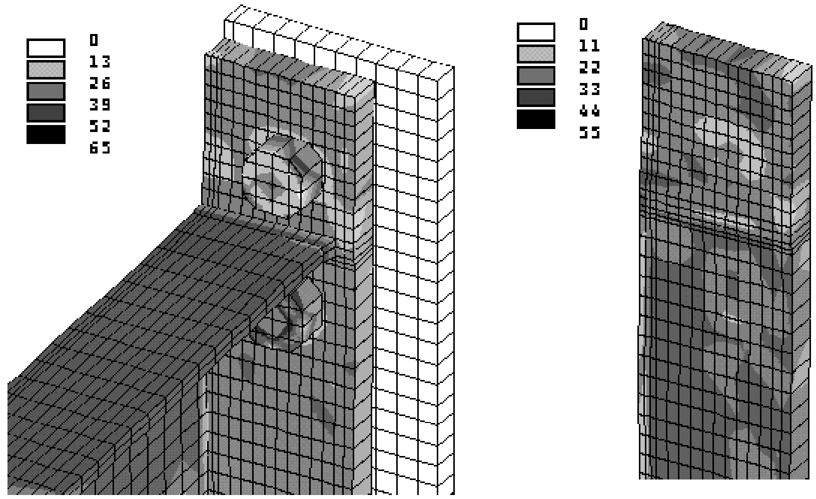

Figure 7: Von Mises stress (ksi) distribution for 4E-1 1/4-1 1/8-24

Figure 8 shows nearly identical relationships for the measured and finite element method predicted applied moment versus end-plate separation curves. Figure 9 compares experimental and finite element method predicted bolt forces as a function of applied moment. As expected, the monitored exterior bolt yielded before the monitored interior bolt. The exterior portion of the end-plate is less stiff than the interior portion and therefore exterior bolt forces tend to be greater because of larger prying forces. These results indicate that, indeed, the finite element method may possibility be used to qualify other end-plate connection configurations for use in seismic lateral force resisting frames.

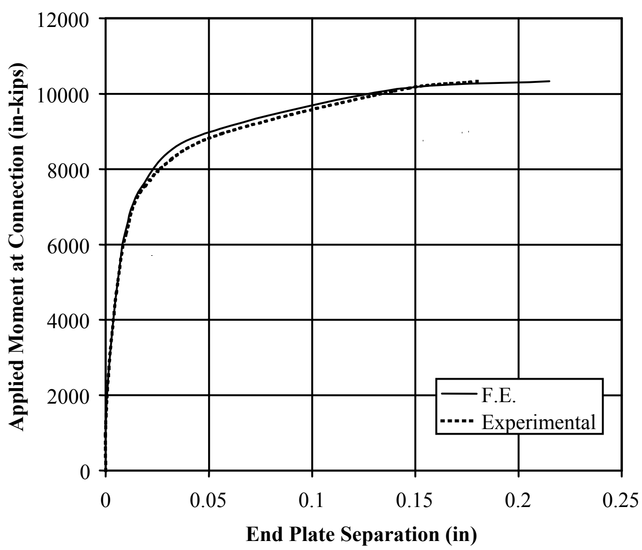

Figure 8: Applied moment vs. end plate separation for 4E-1 1/4-1 1/8-24

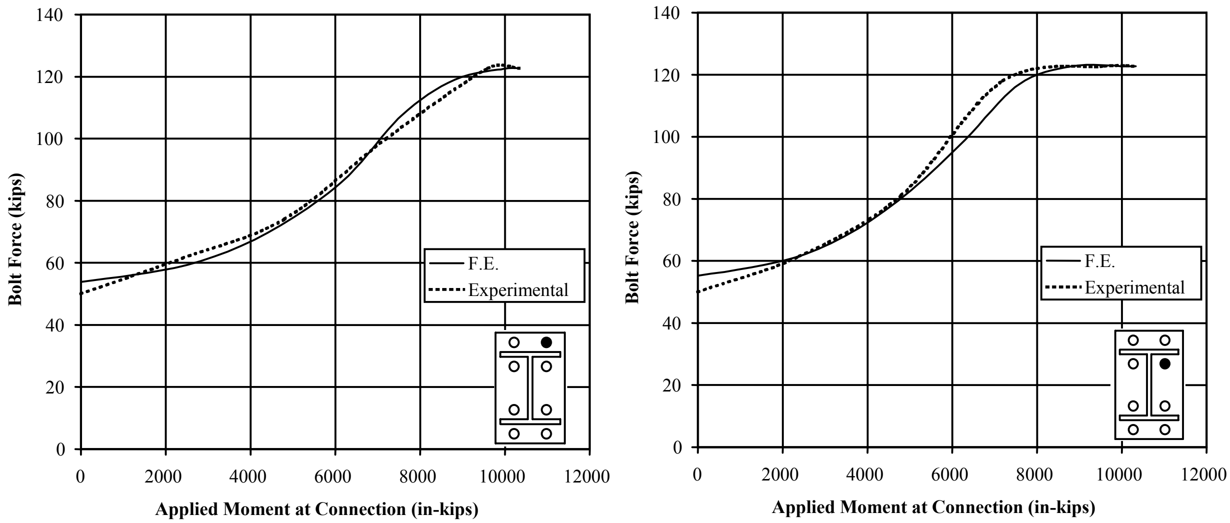

a) Outside bolt b) Inside bolt

Figure 9: Bolt force vs. applied moment for 4E-1 1/4-1 1/8-24

SUMMARY

The results of the six extended moment end-plate connection test indicated that the four bolt unstiffened and eight bolt stiffened extended moment end-plate connections can be designed to withstand cyclic loading and are suitable for use in seismic force resisting moment frames. The strong plate connections exhibited the most ductility while the weak plate connection typically failed in a brittle manner. Results from the test conducted with a composite slab, indicates that the effects of the slab should be considered in the design of the connections. The results from the finite element modeling indicate that the finite element method can be used to predict the behavior of end-plate connections. Additional details and discussion of the extended moment end-plate connection testing completed as a part of the SAC Steel Project can be found in Sumner *et al* (10).

ACKNOWLEDGMENTS

Funding for this research was provided by the Federal Emergency Management Agency through the SAC Joint Venture. SAC is a partnership of the Structural Engineers Association of California, the Applied Technology Council, and California Universities for Research in Earthquake Engineering. Appreciation is extended to FEI Limited and Cives Steel Company for their donation of labor for the fabrication of the test specimens and to PSI, Inc for the donation of welding inspection services. Appreciation is also extended to Nucor-Yamato Steel Company and The Lincoln Electric Company for the donation of test materials.

NOTATION

F_u = specified minimum tensile strength
F_y = specified minimum yield stress
in. = inch, inches
ksi = kips per square inch
rad = radians
vs. = versus
Z_x = plastic section modulus

REFERENCES

1. SAC (1997). *Protocol for Fabrication, Inspection, Testing and Documentation of Beam-Column Connection Tests and Other Experimental Specimens*, Report No. SAC/BD-97/02, SAC Joint Venture.
2. Murray, T. M., (1988). "Recent Developments for the Design of Moment End-Plate Connections," *Journal of Constructional Steel Research*, Vol. 10, pp. 133-162.
3. Kennedy, N. A., Vinnakota, S., Sherbourne, A. (1981). The split-tee analogy in bolted splices and beam-column connections, *Joints in Structural Steelwork*, John Wiley and Sons, New York, pp. 2.138-2.157.
4. Murray, T. M., (1990). *AISC Design Guide Extended End-Plate Moment Connections*, American Institute of Steel Construction, Chicago.
5. AISC (1994). *Load and Resistance Factor Design Manual of Steel Construction*, American Institute of Steel Construction, Chicago.
6. AISC (1997). *Seismic Provisions for Structural Steel Buildings*, American Institute of Steel Construction, Chicago.
7. AWS (1998). *Structural Welding Code - Steel AWS D1.1-98*, American Welding Society, Miami.
8. Meng, R. L. and Murray, T. M. (1997). "Seismic Performance of Bolted End-Plate Moment Connections," *Proceedings of the 1997 National Steel Construction Conference, Chicago, Illinois,* AISC, May 7-9, 1997, 30-1 – 30-14.
9. Mays, T. W., (2000). *Application of the Finite Element Method to the Seismic Design and Analysis of Large Moment End-Plate Connections*, Ph.D. Dissertation, Virginia Polytechnic Institute and State University, Blacksburg, Virginia.
10. Sumner, E. A., Mays, T. W. and Murray, T. M., (2000). "Cyclic Testing of Bolted Moment End-Plate Connections," Research Report SAC/BD-00/21, CE/VPI-ST 00/03, Department of Civil and Environmental Engineering, Virginia Polytechnic Institute and State University, Blacksburg, Virginia.